

Article

Structural and Surface Modification of Oxalic-Acid-Activated Bentonites in Various Acid Concentrations for Bleaching Earth Synthesis—A Comparative Study [†]

Danai Tsakiri , Iliana Douni  and Maria Taxiarchou 

Laboratory of Metallurgy, Department of Mining and Metallurgical Engineering, National Technical University of Athens, 9, Iroon Polytechniou Street, 157 80 Zografos, Greece; douni@metal.ntua.gr (I.D.); taxiarch@metal.ntua.gr (M.T.)

* Correspondence: dtsakiri@metal.ntua.gr

[†] This paper is an extended version of our paper presented at the International Conference on Raw Materials and Circular Economy (RawMat 2021).

Abstract: The aim of this study is to investigate the oxalic acid activation of bentonites containing different types of smectites, analyse their surface modification as a function of acid concentration and create good quality bleaching earths. In particular, two different bentonite samples (one containing aluminum and one containing ferruginous smectite), after being characterized through XRD, XRF and FT-IR analysis, are treated with oxalic acid at a concentration of 0.5, 0.7 and 1 M. Their structural modifications after treatment are observed through FT-IR spectra and surface area and porosity measurement (using the BET equation and the BJH method, respectively) combined with the determination of the main structural metals' extraction from them (using an atomic adsorption spectrometer). The results showed that the ferruginous smectite is more susceptible to oxalic acid activation compared to the aluminum smectite, and all the final products have developed extra porosity in their structure while retaining the structure of smectite (even at 0.5 M acid concentration). The activated samples were used as bleaching earths in soybean oil, and the results proved that Lovibond yellow and red colours as well as the chlorophyll of oil (measured spectrophotometrically) were reduced to the values set by the specifications.

Keywords: acid activation; oxalic acid; smectites; bleaching earths; FT-IR



Citation: Tsakiri, D.; Douni, I.; Taxiarchou, M. Structural and Surface Modification of Oxalic-Acid-Activated Bentonites in Various Acid Concentrations for Bleaching Earth Synthesis—A Comparative Study. *Minerals* **2022**, *12*, 764. <https://doi.org/10.3390/min12060764>

Academic Editor: Dong Liu

Received: 29 April 2022

Accepted: 14 June 2022

Published: 16 June 2022

Publisher's Note: MDPI stays neutral with regard to jurisdictional claims in published maps and institutional affiliations.



Copyright: © 2022 by the authors. Licensee MDPI, Basel, Switzerland. This article is an open access article distributed under the terms and conditions of the Creative Commons Attribution (CC BY) license (<https://creativecommons.org/licenses/by/4.0/>).

1. Introduction

Bentonites are commonly used industrial clays which are mainly composed of smectites. Smectites are a group of minerals with 2:1 structure (two silicon tetrahedral sheets combined with one aluminum octahedral sheet). They are classified according to the cations occupying the tetrahedral and octahedral sites (montmorillonite, nontronite, beidellite, saponite and hectorite). Smectites are characterized by adsorptive and catalytic properties, and many researchers are involved in their study. Their physical and chemical properties depend on their surface area characteristics, the extent and nature of which can be suitably treated and modified. This treatment can be physical or chemical, with acid activation being one of the most common chemical treatments applied to them [1,2]. Acid activation is usually carried out with inorganic acids, such as HCl and H₂SO₄, targeting surface characteristic modification so as to mainly increase the specific surface area and to modify the porosity and surface acidity of the smectite [3–6].

Acid activation of smectites using inorganic acids has been extensively studied.

A number of researchers have investigated the influence of hydrochloric acid on smectites, noticing the creation of a silica phase in the final product. Acid activation of montmorillonite using HCl revealed that activation with acid of 1 to 4 M led to the detachment of layers, the progressive destruction of the octahedral sheet and the initial destruction

of the tetrahedral sheets. In higher concentrations (5 to 6 M), the tetrahedral sheets were completely destroyed, and large quantities of silica were formed and consequently were precipitated on the pores [7]. Other researchers studied the acid activation of smectite with HCl at a constant concentration of 5.3 M for 2–24 h. As it was observed, initially the Na and Ca of the interlayer space were exchanged with H^+ , followed by the dissolution of smectite. FT-IR spectra showed that during acid activation, a significant degradation of the 2:1 structure occurred, which led to the creation of silica phases. The octahedral Al, Fe and Mg were extracted gradually in the solution, and the solid sample was enriched with Si [8]. A comparative study of acid activation with HCl between two different types of smectites (trioctahedral and dioctahedral), investigating the effect of different parameters such as acid concentration, temperature and retention time, revealed that trioctahedral smectite is more prone to acid activation compared to dioctahedral smectite. Moreover, the dissolution rate of smectites was increased with higher contents of Fe and Mg in the octahedral sheets (having substituted Al), as with higher temperature and acid concentration. The material produced after acid activation of both smectites is a hydrous amorphous silica phase [9].

Some studies also dealt with the activation of smectites with sulphuric acid. Isothermal activation of smectite with sulphuric acid of 3 to 5 M, at different temperatures, and 10% pulp density was investigated, suggesting a kinetic model for isothermal sulphuric acid activation based on the results. The activation energy was decreased with increasing the acid concentration, which indicates that the mechanism of structural changes varies depending on the acid concentration. As the acid concentration increases, the specific surface area increases and the activation energy decreases [10]. Structural modifications of montmorillonite during acid activation with sulphuric acid of 1 to 10 N, at 80 °C, for 4 h were studied by using FT-IR spectroscopy. Sulphuric acid affects initially the octahedral sheets of the mineral, leading to the dissolution of octahedral cations. The tetrahedral sheets were observed to be affected by high concentration sulphuric acid. Moreover, Brønsted acid sites were created during the acid activation [11].

Studies dedicated to the activation of silicate minerals with organic acids have shown that treatment with organic acids enhances the dissolution of silicate minerals compared to treatment with inorganic ones due to the complexes formed between organic ligands and metals [12–14]. Several studies dealt with the treatment of smectites with organic acids, in which oxalic acid appears to be more efficient than other organic acids [15–17]. Moreover, the effluents of oxalic acid activation are more environmentally friendly than those from inorganic acids due to their ability to be decomposed microbiologically and photochemically [18]. Taking into consideration the abovementioned points, oxalic acid could be an effective agent for smectite activation.

Recently, oxalic acid activation of smectites has been investigated by a number of researchers as a promising alternative method for their surface modification to create bleaching earths. Smectites from Greece were treated with oxalic acid in order to study the effects of temperature, pulp density and retention time on the bleaching properties of the mineral [18]. The optimum results were obtained with 1 M oxalic acid, pulp density 25%, at 100 °C. A study on the activation of montmorillonite with oxalic acid at 25 °C revealed that dissolution is enhanced in the presence of oxalic acid (pH 4–8) in comparison with ligand-free solutions (composed of nitric, acetic and hydrochloric acid to control the pH) due to the formation of oxalate surface complexes and soluble chelates. Useful information on the oxalate complexes was provided through the FT-IR method [19]. Based on the results of the above study, the researchers modelled the complexation of oxalate on the edge surface of montmorillonite [20].

Acid activation of smectites is of paramount importance for the vegetable oil industry since the activated materials produced constitute the bleaching earths which are used in oil refining [21].

Vegetable oils occupy the third place in world food consumption after cereals and rice [22]. Among vegetable oils, soybean oil, palm oil, rapeseed oil and sunflower oil predominate in world oil production and exports. In their crude form, they contain undesirable

compounds and impurities which must be removed through the refining process. Bleaching is an essential step of this process during which chlorophyll is removed, peroxides are decomposed and other compounds such as soaps, metal cations and nonhydratable phospholipids are reduced by using a bleaching earth as an adsorbent. Inorganic-acid-activated calcium montmorillonite is the main material used as a bleaching earth in the industry of edible oils [23]. The bleaching efficiency of raw and activated smectite in soybean oil was assessed through the calculation of red colour of the oil before and after bleaching, showing its dependence on the mesopore size distribution [24]. The optimization of acid activation of smectite in order to improve its bleaching capacity in colza oil was studied. Chlorophyll content and colour of oil were measured for the evaluation of results, which proved that acid concentration and retention time affected the bleaching power of smectite [25].

The existing literature includes a variety of studies on the conventional inorganic acid activation of smectites. A limited amount of information has been collected so far on the organic, and more specifically the oxalic, acid activation of smectites. These studies developed a comprehensive understanding of the kinetics and the mechanism that controls smectite dissolution in oxalic acid systems. Kinetic studies about oxalic acid activation deal with the observation of the release of a specific metal from the structure of smectite versus various parameters. Moreover, the studies on the activation mechanism concern smectite dissolution in oxalic acid under mild conditions and the complexes formed due to the presence of oxalic acid. However, studies related to the use of oxalic-acid-activated smectites in industrial applications, such as the decolourization of edible oils during the refinement process, are limited.

The present work is a comparative study of the oxalic acid activation of two different types of bentonites (one containing aluminum smectite and one containing a ferruginous one) using various elevated acid concentrations. The bleaching efficiency of oxalic-acid-activated bentonites was tested in soybean oil and correlated to the structural modifications of the materials. It was proved that oxalic acid activation is an appropriate technique for the modification of textural and surface properties of bentonites in order to improve their adsorption capacity.

The study aims to; (a) investigate the effect of oxalic acid on bentonites containing different types of smectites (aluminum and ferruginous) since the dissolution is expected to diverge depending on the occupancy of octahedral sites of smectites; (b) analyse the porosity and surface alteration of materials as a function of oxalic acid concentration; (c) evaluate the bleaching capacity of the oxalic acid activated bentonites and to correlate it to the porosity of the materials produced.

2. Materials and Methods

Two different raw bentonites, one containing an aluminum smectite from the deposits of Milos Island in Greece and one containing a ferruginous smectite from Gujarat in India, were provided by IMERYS S.A. and labelled as AlBe-G and FeBe-I, respectively. The chemical analysis of the raw materials was performed by the XRF method using a XEPOS apparatus of SPECTRO company. FTIR spectra of solid samples were obtained in the 400–4000 cm^{-1} range using a Perkin Elmer Spectrum 100 Fourier Transform Infrared (FTIR) spectrometer and the KBr pellet technique. The samples' mineralogical compositions were determined using a Bruker D8-Focus X-ray Diffractometer with nickel-filtered CuK α radiation ($\lambda = 1.5406 \text{ \AA}$) at 40 kV and 40 mA.

The leachates of the acid activation process were analysed regarding their Al, Si, Fe and Mg contents through atomic absorption spectrometry using a Perkin Elmer PinAAcle 900T Atomic Absorption Spectrometer.

The specific surface area and porosity of the samples were analysed through the BET equation, the BJH method and the 50-point N $_2$ adsorption/desorption isotherms, obtained by a Quantachrome Autosorb IQ surface area and pore size analyser.

FT-IR spectra were also obtained for the acid activated samples, using the KBr pellet technique, in a range from 400 to 4000 cm^{-1} with 4 cm^{-1} resolution. This technique is a

very sensitive one and can be used to observe the structural modifications occurring during the acid activation of the smectite samples.

The activated bentonites were used as bleaching earths for the decolourization of soybean oil, which was provided by ELAIS Unilever Hellas S.A. Chlorophyll, and Lovibond colour was measured in the oil before and after each bleaching test using a spectrophotometric method based on AOCS Cc13i-96 and the BS 684-1-1.14:1987 method.

Batch oxalic acid activation experiments were carried out in a glass reactor with a heating jacket. A pulp density of 2% (*w/v*) was obtained by placing 8 g of solid in 400 mL of oxalic acid solution of 0.5, 0.7 and 1 M concentrations. The temperature remained constant at 80 °C using a Teflon-coated thermocouple connected to the temperature controller. The reactor was sealed, and a glass condenser was adjusted to it in order to avoid vapour losses. The pulp was mechanically stirred at 400 rpm for 24 h, and 5 mL samples were collected at 10 min, 20 min and 30 min at the beginning of the process and then every hour. Finally, the pulp was filtrated and the solid residue on the filter was washed with deionized water and dried at 100 °C for 24 h.

The bleaching efficiency of the oxalic-acid-activated bentonites produced was evaluated through bleaching tests using soybean oil. The bleaching tests were carried out in a spherical glass reactor with a heating mantle. A coated thermocouple connected to a temperature controller was used to keep the temperature constant at 80 °C. At that temperature, the bleaching earth was added to the oil at a solid/oil ratio of 3% (*w/w*) and remained in the oil for 30 min under mechanical stirring (at 250 rpm). After the test, the bleached oil was filtered in order to measure its Lovibond colour and chlorophyll content. Furthermore, one more bleaching test was carried out using the commercial bleaching earth known as “Tonsil” (bleaching earth used by the vegetable oil industry), which was provided by ELAIS Unilever Hellas S.A., in order to compare the bleaching earths of the present study with a commercial one.

3. Results and Discussion

3.1. Characterization of Raw Materials

3.1.1. Chemical Analysis of Raw Materials

Table 1 presents the chemical composition of each raw bentonite sample, measured by the XRF method. AlBe-G has lower content of Na₂O and higher content of CaO compared to FeBe-I. The exchangeable cations (Ca²⁺, Na⁺, Mg²⁺ and K⁺) were determined and the ratio $\Sigma (K^+ + Na^+) / \Sigma (Ca^{2+} + Mg^{2+})$ was calculated at about 0.1 for AlBe-G and 0.5 for FeBe-I. Moreover, the swelling index of the AlBe-G sample is $3.985 \times 10^{-3} \text{ m}^3/\text{kg}$, while that of the FeBe-I sample is $7.6 \times 10^{-3} \text{ m}^3/\text{kg}$ (which is in accordance with the higher Na₂O content of FeBe-I compared to AlBe-G). The above observations led to the assumption that the smectite of FeBe-I falls within the classification of mixed Na/Ca smectite and the one of AlBe-G within that of Ca-smectite [26,27].

Table 1. Chemical Analysis of raw materials.

	Oxides (wt.%)									Total
	SiO ₂	Al ₂ O ₃	Fe ₂ O ₃	MgO	CaO	Na ₂ O	K ₂ O	TiO ₂	L.O.I.	
AlBe-G	48.28	17.25	3.68	5.28	9.01	0.40	0.30	0.71	15.10	100.00
FeBe-I	46.96	17.66	19.32	2.80	1.75	1.08	0.00	1.39	9.05	100.00

3.1.2. X-ray Diffraction of Raw Materials

The XRD spectra and the mineralogical compositions of the two raw materials are presented in Figure 1a. The main peaks belong to montmorillonite, and based on the results, it is assumed that this is the main mineral phase. The AlBe-G sample contains calcite, dolomite and illite, while the FeBe-I sample contains kaolinite, hematite, calcite and calcium titanium oxide.

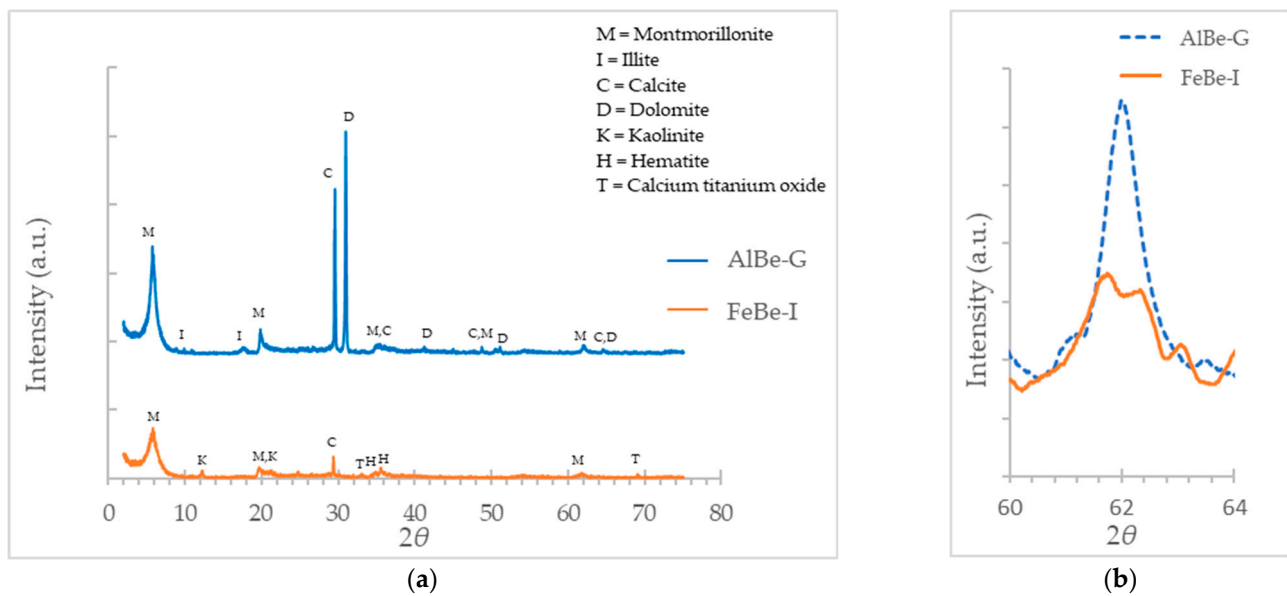


Figure 1. X-ray diffraction of raw materials (a) full diagram (b) 060 regions.

The occupancy of the octahedral sheets by Al or Fe in phyllosilicates is observed in 060 reflection in the XRD spectrum. For Fe-containing dioctahedral 2:1 clays, such as nontronite, the 060 maximum is located at a lower 2θ compared to Al-containing ones (such as montmorillonite) [28]. Taking into consideration the 060 maximum of the AlBe-G sample, which is located at higher 2θ values than that of the FeBe-I sample (Figure 1b), it can be deduced that the smectite of FeBe-I is a Fe-containing one and that of AlBe-G is an Al-containing one.

FeBe-I smectite could be assigned as nontronite taking into consideration the high iron content of the sample and the smectite peaks of the XRD spectra. Nevertheless, this interpretation is not valid, as it is indicated by the d_{060} value. According to the correlation of the number of octahedral Fe ions in nontronites and Fe-rich smectites with their d_{060} values (presented graphically in a previous study [29]), the FeBe-I sample contains a ferruginous smectite and not a nontronite since its d_{060} value is equal to 1.50 Å.

3.1.3. Infrared Spectroscopy of Raw Materials

The full FT-IR spectra of the AlBe-G and FeBe-I samples are presented in Figure 2. In the spectrum of the AlBe-G sample, the characteristic band of Si-O stretching vibrations of the tetrahedral layer is the most intensive one, and the bands attributed to Si-O-Al (octahedral) and Si-O-Si bending vibrations are observed at the lowest wavelengths (524 and 468 cm^{-1} , respectively). The peaks assigned to AlAlOH, AlFeOH and AlMgOH, which are located at 918 cm^{-1} , 881 cm^{-1} and 845 cm^{-1} , respectively, indicate that aluminum is partially substituted by iron and magnesium in the octahedral sheets. A band appears at 627 cm^{-1} due to perpendicular vibration of the octahedral atoms (R-O-Si), which is also characteristic of Al-rich montmorillonites [30]. In addition, the bands from 1382–1430 cm^{-1} in the raw sample are related to CO_3 stretches of calcite and dolomite, and the one noticed from 710–715 cm^{-1} is assigned to Si-O stretching and the in-plane bending of calcite and dolomite [31].

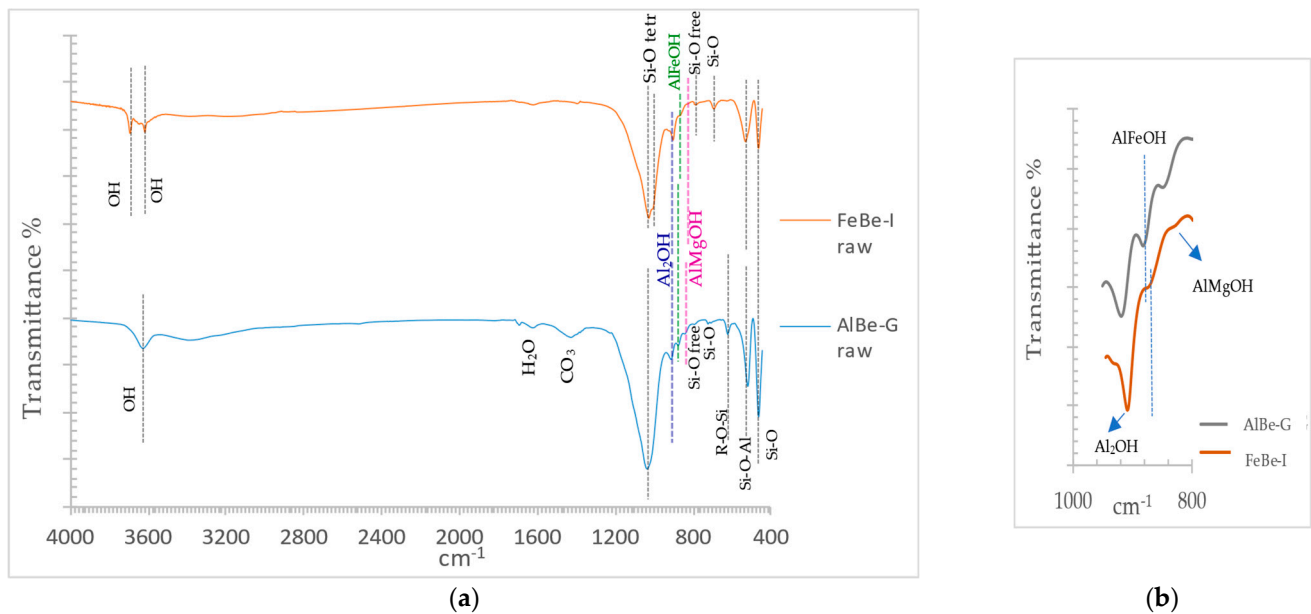


Figure 2. FT-IR spectra of raw materials. (a) Full spectra; (b) section 1000–800 cm^{-1} .

In the FeBe-I sample's spectrum, the bands at 1030 cm^{-1} and 1012 cm^{-1} are assigned to the Si-O stretching band [9]. As in the AlBe-G sample, the Si-O-Al and Si-O-Si bending vibration bands are observed at 535 cm^{-1} and 468 cm^{-1} , respectively, while the Al_2OH , AlFeOH and AlMgOH peaks appear at 907, 874 and 832 cm^{-1} , respectively. The bands at 3623 cm^{-1} and 3696 cm^{-1} are assigned to hydroxyl groups joined together with octahedral atoms.

In Figure 2b, the position of the peak assigned to AlFeOH (a good indicator of the octahedral aluminum abundance) is presented. According to Goodman et al. [32], this peak shifts from 847–851 cm^{-1} for smectites with relatively low quantity of aluminum in the octahedral sheets (nontronites) up to 873–890 cm^{-1} for smectites with the highest Al content in the octahedral sheets (montmorillonites). As they concluded, the AlFeOH librational vibration is located at higher frequencies in the case of aluminum-neighbouring atoms, while it appears at lower frequencies in the case of iron atoms, leading to the assumption that in the FeBe-I sample, iron predominates among the octahedral atoms, while in the AlBe-G sample, aluminum occupies the main octahedral sites.

The peaks at 3623, 3696 cm^{-1} , 913, 876 and 468 cm^{-1} for FeBe-I raw material, confirm the assumption that smectite mineral of FeBe-I sample is not considered as a nontronite [33].

The XRD and FTIR diagrams of the samples in relation to the abovementioned literature provided useful information about the type of smectite contained in each sample. Observing the 060 maximum in the XRD diagrams, it was indicated that FeBe-I contains mainly octahedral iron, while AlBe-G contains mainly octahedral aluminum. To the same assumption leads the position of librational vibration of AlFeOH in IR spectra, which is located at lower frequencies for FeBe-I compared to AlBe-G. Those conclusions from XRD and IR diagrams revealed that FeBe-I contains a ferruginous smectite and AlBe-G an aluminium one.

3.2. Metals' Extraction during Acid Activation of Samples

Figure 3 presents the extraction percentage for each metal during the acid activation of each sample versus time and oxalic acid concentration. The extraction percentage is calculated as seen below:

$$\%E = \frac{m_l}{m_s} \times 100$$

where %E is the percentage of extraction for each metal, m_l is the mass of metal extracted in the oxalic acid solution and m_s is the mass of metal in the initial solid sample. The metals'

extraction diagrams (Figure 3) depict that the amount of metal extracted increases over time. However, the extraction percentage of silicon reduces after 2 h, which shows that Si is precipitated. The figure also reveals that there is no significant effect on the dissolution of AlBe-G as the acid concentration changes from 0.5 to 1 M.

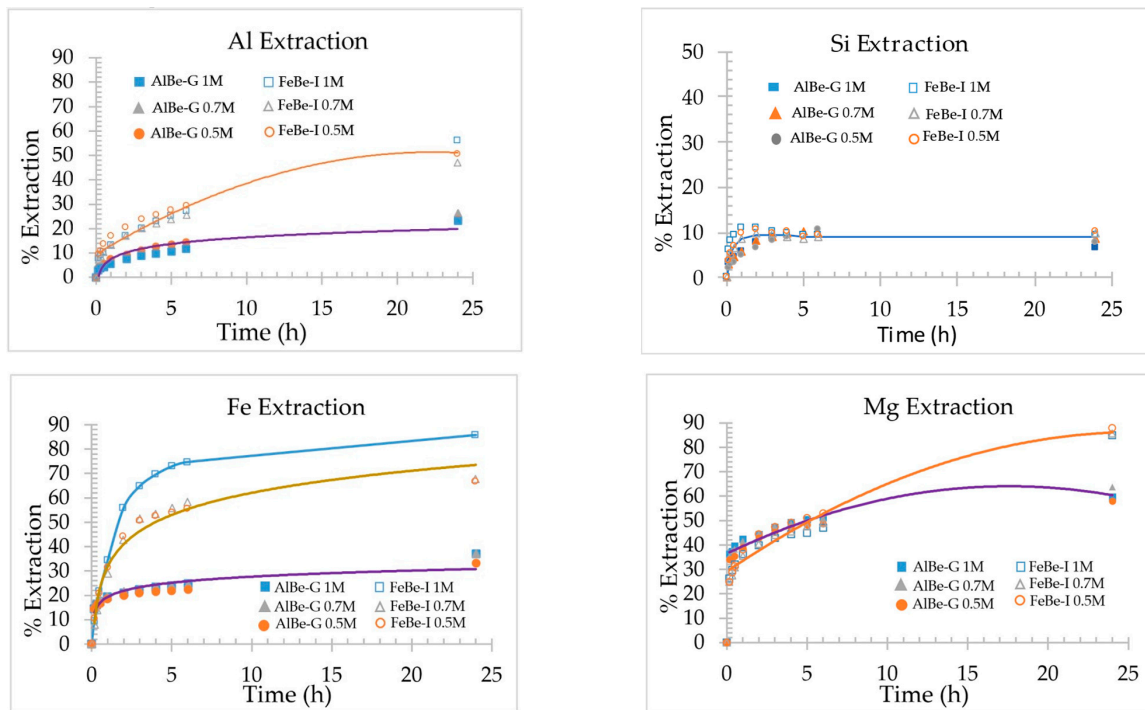


Figure 3. Extraction of metals versus time for AlBe-G and FeBe-I samples in oxalic acid (80 °C; acid concentrations of 0.5 M, 0.7 M and 1 M; 2% of pulp density).

3.3. Oxalic Acid Activated Aluminum Smectite

Figure 4 presents the FT-IR spectra of the raw and activated AlBe-G samples.

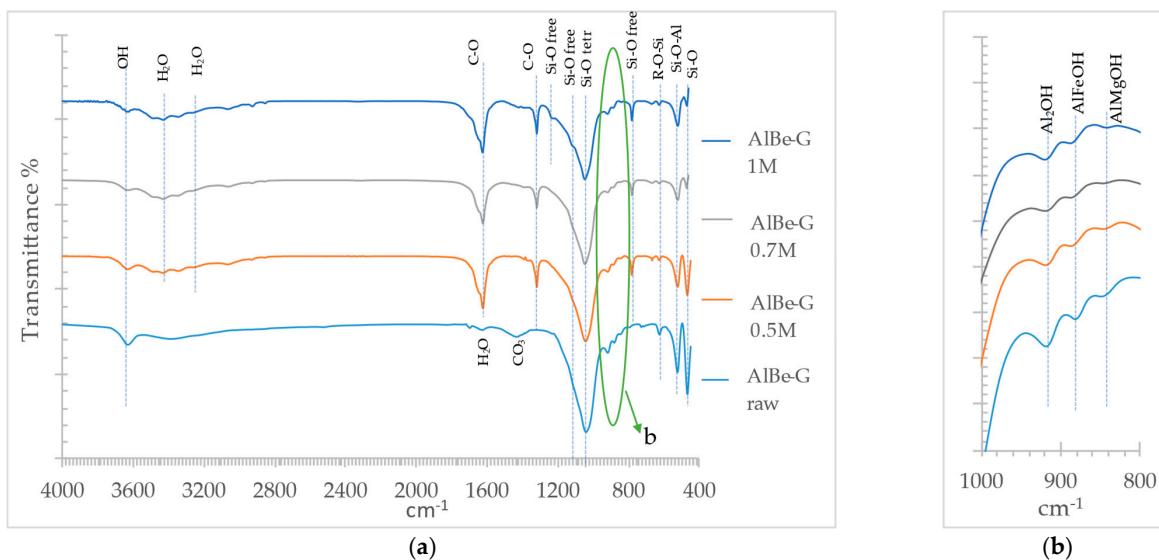


Figure 4. FT-IR spectra of AlBe-G samples (raw and activated with 0.5, 0.7 and 1 M oxalic acid). (a) Full spectra; (b) section 1000–800 cm⁻¹.

The leaching caused by the oxalic acid treatment affects the bands at 3625 cm⁻¹, 627 cm⁻¹, 524 cm⁻¹ (Figure 4a), 918 cm⁻¹, 881 cm⁻¹ and 845 cm⁻¹ (Figure 4b), confirming

the depletion of the octahedral atoms. The band at 3625 cm^{-1} , which is assigned to hydroxyl groups joined together with octahedral Al, decreases when the sample is treated with oxalic acid [11]. Furthermore, the three peaks in the hydroxyl bending region for Al_2OH , AlFeOH and AlMgOH also decrease (with the AlMgOH peak becoming the smoothest) due to the extraction of octahedral atoms. Obtained IR vibrations indicate that the octahedral structure is preserved (Figure 4b). This is confirmed by the extraction diagrams, which indicate that the octahedral atoms are leached out from the mineral during treatment, reaching an extraction of 25% for Al, 35% for Fe and 60% for Mg (Figure 3).

Moreover, the band at 524 cm^{-1} (indicative of the extent of smectite dissolution) is still visible and—along with the bands of octahedral atoms and tetrahedral Si—reveals that the smectite structure still exists even after activation at 1 M concentration.

A small shift of the Si-O band (1040 cm^{-1}) to a higher wavelength, combined with its decreasing intensity after treatment, indicates a low decomposition of the structure. Precipitation of Si is confirmed by the presence of amorphous silica bands at 1200 cm^{-1} and 1100 cm^{-1} as Si-O free, prominent at 1 M concentration and near 800 cm^{-1} in every studied concentration (Figure 4a) [9].

Two peaks assigned to calcium oxalate appear in the activated samples. These peaks correspond to one vibration at 1624 cm^{-1} for the asymmetric $\nu_a(\text{CO})$ and one vibration at 1320 cm^{-1} for the symmetric $\nu_s(\text{CO})$ of the oxalate group [34].

The surface area and porosity of the AlBe-G samples are presented in Table 2. They are considered mesoporous materials based on IUPAC classification since their average pore diameter is about 51 to 66 Å [35]. Porous materials with much higher specific surface areas and pore volumes compared to the raw bentonite are produced after acid activation due to the leaching of structural cations of smectite [36]. The average pore diameter of the treated samples (about 51 to 54 Å) decreases compared to that of the raw one. The specific surface area and pore volume have an upward trend as the acid concentration increases, while they stabilize after 0.7 M (Figure 5).

Table 2. Specific surface area and porosity of raw and treated AlBe-G bentonite ($80\text{ }^\circ\text{C}$; acid concentrations of 0.5 M, 0.7 M and 1 M; 2% of pulp density).

	AlBe-G Raw	AlBe-G 0.5 M	AlBe-G 0.7 M	AlBe-G 1 M
Specific surface area (m^2/g)	28.11	128.37	175.04	169.13
Average pore diameter (Å)	65.98	54.10	51.41	54.84
Total pore volume (cm^3/g)	0.046	0.174	0.225	0.232

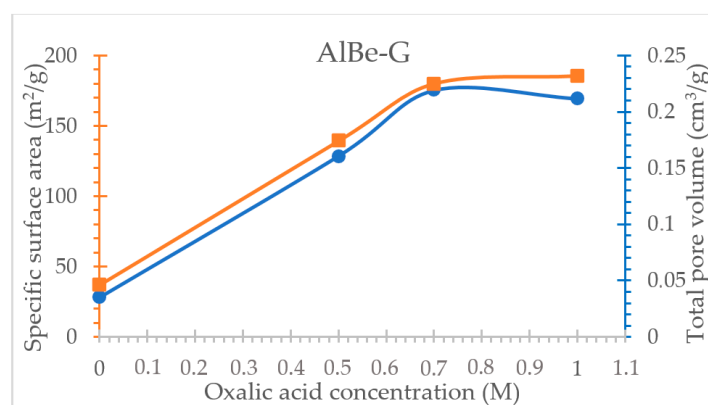


Figure 5. Specific surface area and total pore volume diagram of raw (labelled as “0” in the horizontal axis) and treated AlBe-G bentonite ($80\text{ }^\circ\text{C}$; acid concentrations of 0.5 M, 0.7 M and 1 M; 2% of pulp density).

The pore size distribution of raw and activated AlBe-G material is presented in Figure 6. It is apparent that the activated materials have higher number of pores within a wider range of sizes.

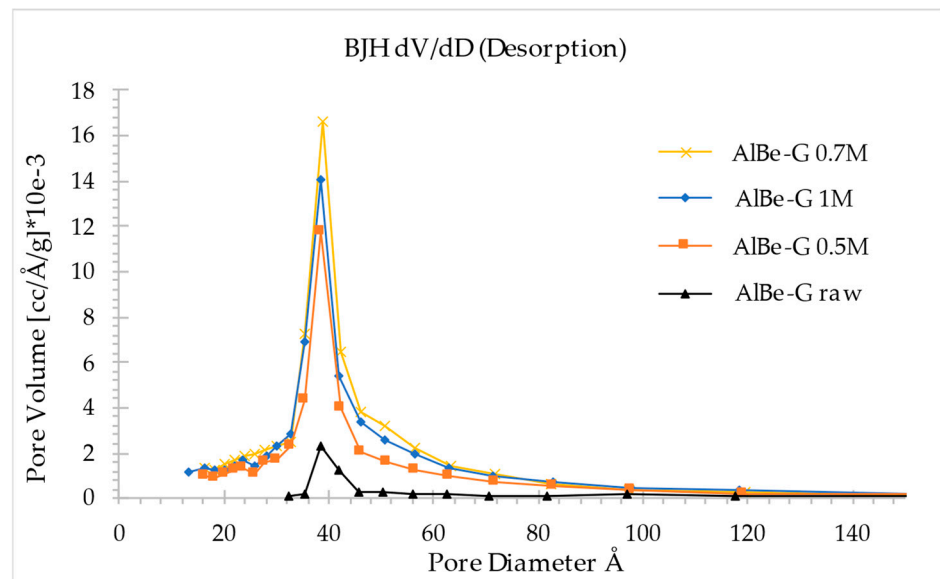


Figure 6. Pore size distribution of AlBe-G samples (80 °C; acid concentrations of 0.5 M, 0.7 M and 1 M; 2% of pulp density).

3.4. Oxalic Acid Activated Ferruginous Smectite

In the FT-IR spectra of the FeBe-I raw and activated samples (Figure 7a), the bands at 1030 cm^{-1} and 1012 cm^{-1} are assigned to the Si-O stretching band [9]. There are also two bands for calcium oxalate at 1627 cm^{-1} and 1318 cm^{-1} .

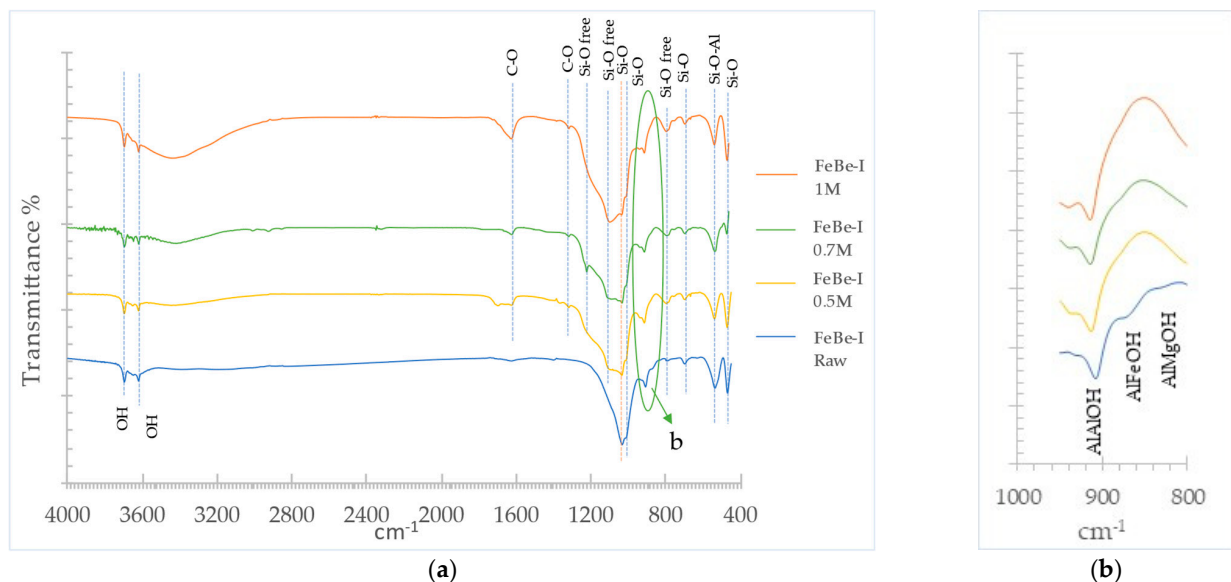


Figure 7. FT-IR spectra of FeBe-I smectite (raw and activated with 0.5, 0.7 and 1 M oxalic acid). (a) Full spectra; (b) section $1000\text{--}800\text{ cm}^{-1}$.

The intensity of the bands at 3623 cm^{-1} and 3696 cm^{-1} reduces with acid treatment due to the removal of the hydroxyl groups connected to the octahedral atoms that are leached out from the smectite structure [11].

The peaks of Al_2OH , AlFeOH and AlMgOH gradually decrease as the acid concentration increases due to the extraction of octahedral atoms. The AlMgOH band disappears

completely after treatment at acid concentrations of 0.5 M or higher, while the AlFeOH disappears with treatment at 1 M (Figure 7b), in contrast to the Al band, which remains intense. These observations are confirmed by the metals' extraction diagrams (Figure 3), where the dissolution of about 90% of Mg and Fe is observed at the aforementioned concentrations.

In the FeBe-I sample, structure alteration is observed through the increasing bands at 1110 cm^{-1} and near 800 cm^{-1} due to the creation of amorphous silica and a small decrease in the octahedral bands. In the treated samples, the bands at 1110 cm^{-1} and 1200 cm^{-1} , which have been assigned to hydrous silica, are more prominent with increasing acid concentration. The intensity of the Si-O stretching band at 1012 cm^{-1} diminishes and the band at 1110 cm^{-1} for amorphous Si-O₂ rises with increasing acid concentration. The band at 1030 cm^{-1} , observed in all acid concentrations, indicates the presence of Si in the tetrahedral structure. Thus, the crystal structure of the mineral has not completely collapsed [8,9].

In this sample, as in the AlBe-G one, the characteristic band at 535 cm^{-1} and the bands referring to octahedral atoms, as well as the principal bands of the smectite structure, still exist. Thus, the crystal structure seems to be preserved even after smectite activation with 1 M acid concentration.

The surface area and porosity of FeBe-I samples are presented in Table 3. Based on IUPAC classification, FeBe-I samples are mesoporous materials since their average pore diameter is about 40 to 46 Å [35]. The specific surface area and total pore volume of FeBe-I bentonite increase after the acid treatment (Table 3) due to the leaching of the structural cations from smectite [36]. They both increase with increasing acid concentration, while the specific surface area obtains a stable value of about $395\text{ m}^2/\text{g}$ at 0.7 and 1 M concentration (Figure 8). The average pore diameter is almost the same in the treated and untreated samples.

Table 3. Specific surface area and porosity of raw and activated FeBe-I ($80\text{ }^\circ\text{C}$; acid concentrations of 0.5 M, 0.7 M and 1 M; 2% of pulp density).

	FeBe-I Raw	FeBe-I 0.5 M	FeBe-I 0.7 M	FeBe-I 1 M
Specific surface area (m^2/g)	63.21	320.16	396.84	394.87
Average pore diameter (Å)	40.20	41.31	40.54	45.72
Total pore volume (cm^3/g)	0.064	0.331	0.402	0.451

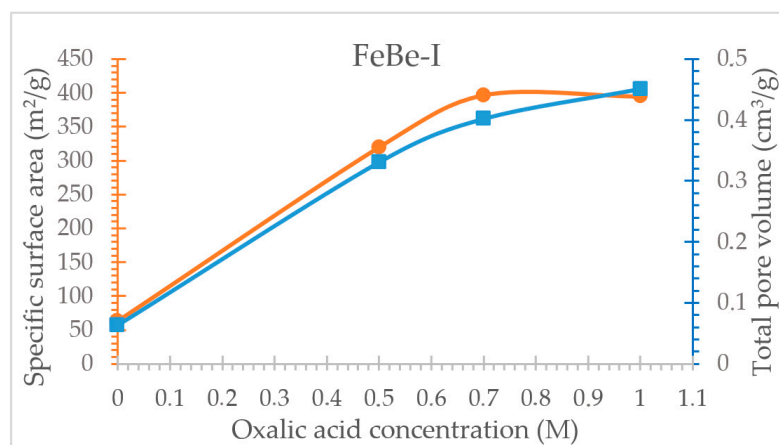


Figure 8. Specific surface area and total pore volume diagram of raw (labelled as "0" in the horizontal axis) and treated FeBe-I samples ($80\text{ }^\circ\text{C}$; acid concentrations of 0.5 M, 0.7 M and 1 M; 2% of pulp density).

The pore size distribution of raw and activated FeBe-I bentonites is presented in Figure 9. The untreated sample has a lower and narrower distribution of pores. As the concentration rises, the distribution of pores expands within a wider range of sizes.

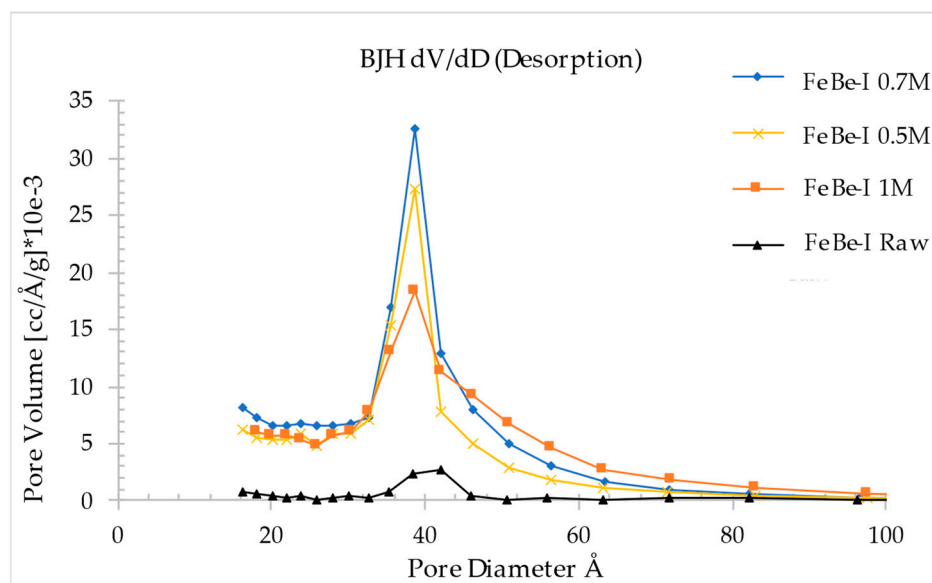


Figure 9. Pore size distribution of FeBe-I (80 °C; acid concentrations of 0.5 M, 0.7 M and 1 M; 2% of pulp density).

3.5. Bleaching Efficiency of Oxalic Acid Activated Bentonites

The oxalic-acid-activated AlBe-G and FeBe-I samples were used as bleaching earths for the bleaching of soybean oil. Their bleaching efficiency was assessed by measuring the chlorophyll content and Lovibond colour of the bleached oil. The results were compared with the values of the untreated oil and those of bleached oil, using “Tonsil” as bleaching earth. The tables below present the abovementioned values (Tables 4 and 5).

Table 4. Chlorophyll content of untreated and bleached oil samples (80 °C, t = 30 min, 250 rpm, 3% w/w).

Bleaching Earth	Chlorophyll (mg/kg)
None	3.90
Tonsil	<0.01
AlBe-G 0.5 M	0.05
AlBe-G 0.7 M	0.03
AlBe-G 1 M	0.03
FeBe-I 0.5 M	0.12
FeBe-I 0.7 M	0.12
FeBe-I 1 M	0.09

As it is observed, chlorophyll is reduced after bleaching soybean oil with all the used bleaching earths. Among all bleaching earths, “Tonsil” presented the highest chlorophyll removal. However, adequate bleaching occurs when chlorophyll is reduced to 0.05–0.09 ppm [37]. Thus, AlBe-G samples activated in oxalic acid of 0.5 to 1 M concentration and FeBe-I activated in 1M seem to sufficiently remove chlorophyll from soybean oil. The soybean oil bleached with activated AlBe-G bentonites contained less chlorophyll than the oil bleached with activated FeBe-I bentonites, as is graphically illustrated in Figure 10, indicating that there is no correlation between specific surface area and chlorophyll removal. This is in accordance with the literature, where bleaching capacity is not associated with

maximum surface area [3]. Pores of either small or large size increase the extent of surface area. However, their diameter may not be large enough for organic molecules, such as chlorophyll or their agglomerates, to fit in [38].

Table 5. Lovibond red and yellow of untreated and bleached oil samples (80 °C, t = 30 min, 250 rpm, 3% w/w).

Bleaching Earth	Lovibond Red	Lovibond Yellow
None	7.3	40.0
Tonsil	4.0	30.0
AlBe-G 0.5 M	5.0	30.0
AlBe-G 0.7 M	3.0	30.0
AlBe-G 1 M	2.3	30.0
FeBe-I 0.5 M	4.0	40.0
FeBe-I 0.7 M	2.0	40.0
FeBe-I 1 M	2.1	30.0

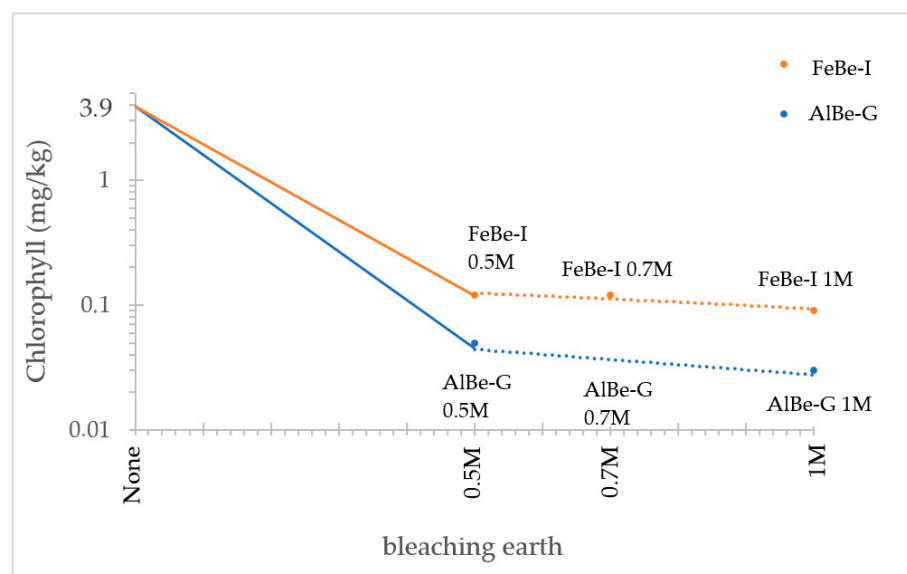


Figure 10. Chlorophyll values before and after bleaching tests with oxalic acid activated bentonites in soybean oil (80 °C, t = 30 min, 250 rpm, 3% w/w).

Lovibond red and yellow (which are associated with carotene content [39]) are also reduced after bleaching compared to untreated oil. It is observed that the oil treated with oxalic-acid-activated bentonites presents lower values of Lovibond red compared to that treated with Tonsil. Furthermore, the results show that as the concentration of oxalic acid during the activation of bentonites increases, the red colour decreases, and consequently, bentonites activated at 1 M oxalic acid are the most efficient in colour reduction (Figure 11).

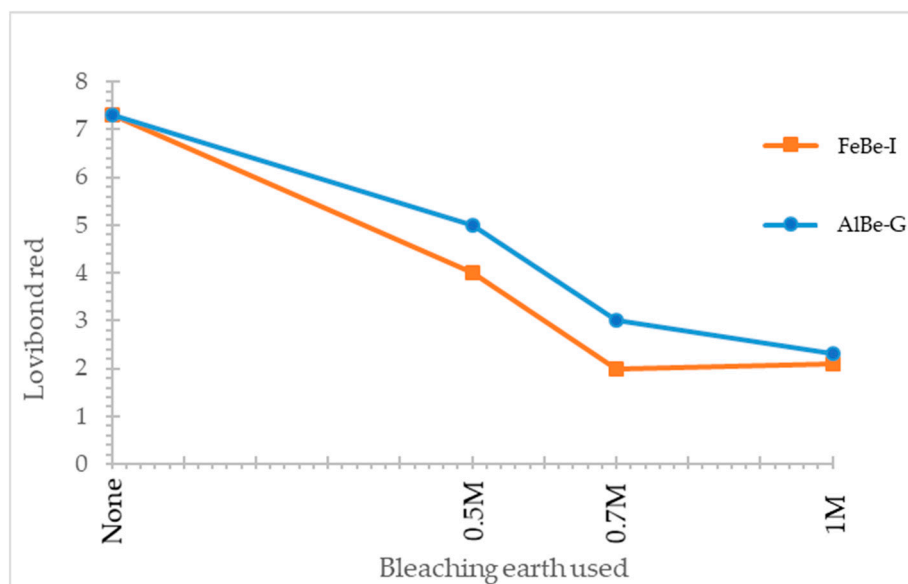


Figure 11. Red colour values before and after bleaching tests with oxalic acid activated bentonites in soybean oil (80 °C, $t = 30$ min, 250 rpm, 3% w/w).

3.6. Comparison of Acid-Activated AlBe-G and FeBe-I Samples

It is apparent from the FT-IR spectra and the metal extraction diagrams of both samples that the octahedral atoms are the first to be leached out from the smectite structure during oxalic acid activation, changing the characteristic absorption bands in the IR spectra. In addition, the tetrahedral sheets are partly dissolved since there is an increase in amorphous silica after the oxalic acid treatment. However, the crystal structure of the minerals has not completely collapsed, and the structure of the activated materials has the form of smectite, even at 1 M concentration [8].

The spectra of AlBe-G and FeBe-I present similar changes (Figures 4a and 7a). However, ferruginous smectite seems to be more prone to dissolution in oxalic acid, as is indicated by the pronounced presence of amorphous silica as well as by the higher extraction of metals compared to AlBe-G (Figure 3). Furthermore, the observation that the FeBe-I is more susceptible to acid attack than AlBe-G is in accordance with a previous study suggesting that smectites with higher Fe content, having substituted Al in the octahedral sheets, are more susceptible to acid attack [9].

Acid concentration has no significant effect on the dissolution of AlBe-G as it increases from 0.5 to 1 M. Oxalic acid (with 0.5 to 1 M concentration) leads to precipitation of free silica and Ca-oxalate, which apparently passivates the surface of the mineral and inhibits the continuation of its dissolution [7]. Moreover, Figure 3 shows that the extraction of metals in FeBe-I is higher than that in the AlBe-G. This is attributed to the much lower Ca content of the first compared to the latter (Table 1) and, consequently, to the lower amount of Ca-oxalate produced. Thus, the inhibition of dissolution caused by precipitation is much reduced, leading to higher metal extraction. The fact that Al and Si are extracted in lower percentages compared to Fe and Mg in both samples shows that oxalic acid selectively leaches out the Fe and Mg from the mineral, creating a porous material which retains the crystal structure of smectite.

It is observed that the products obtained after acid activation of the FeBe-I bentonite are materials with higher specific surface area as well as a higher number of pores with smaller diameter compared to the AlBe-G-activated bentonite. As the concentration increases, the pore volume of acid-treated FeBe-I increases accordingly, while the average pore diameter remains at the same level. The latter occurs due to the selective leaching of Fe and Mg while the structure of smectite is retained. Thus, AlBe-G does not reach as high a pore

volume as FeBe-I due to the fact that AlBe-G has a lower content of Fe in its octahedral sheets compared to FeBe-I.

Bleaching tests revealed that all the products of the present study could be used as bleaching earths since chlorophyll and colour of soybean oil were reduced adequately. The AlBe-G-activated samples removed the chlorophyll more efficiently from soybean oil compared to the FeBe-I-activated ones. Thus, this could be attributed to the average pore diameter of the samples. The average diameter of pores in the AlBe-G samples is about 50–55 Å, whereas in the FeBe-I samples, it is about 40–45 Å. According to the literature [40], the monomeric chlorophyll, which is a common pigment in oils, has a cross-sectional dimension of ca 12×15 Å. Thus, the chlorophyll molecules can partly or wholly enter the pores with radii of 10 Å or less. Consequently, it can be deduced that even though the pores of AlBe-G samples are fewer than those of FeBe-G bentonite, they have the proper diameter for the chlorophyll molecules to fit into.

All the colour values fall within the range of specifications for bleached soybean oil (<5 for red and <50 for yellow [41]) after bleaching with oxalic-acid-activated bentonites. Unlike what occurs with chlorophyll, the removal of colour from the oil does not seem to be dependent on pore diameter. It was observed that both bentonite samples activated at oxalic acid of 1 M concentration decolourized the soybean oil sufficiently. The most efficient decolourization was that of FeBe-I 1 M, which could be attributed to the larger pore volume of this sample.

4. Conclusions

It was observed that the dissolution of bentonites in oxalic acid differentiates according to the atoms occupying the octahedral sheets of smectites. The FeBe-I sample, which contains larger amount of Fe in its octahedral sites than the AlBe-G one, proved to be more susceptible to oxalic acid activation. The amorphous silica peaks of the FeBe-I sample appear to be stronger, and its octahedral atoms are more easily leached out during oxalic acid activation compared to AlBe-G in the same experimental conditions.

The oxalic-acid-activated product appears to be a new material with higher specific surface area compared to the raw material, retaining the structure of smectite but also having enough mesopores in its structure to adsorb other ions or molecules (such as chlorophyll) in its lattice and act as a bleaching earth for edible oils. The colour and chlorophyll measurements in bleached oils confirmed that oxalic-acid-activated bentonites are efficient bleaching earths since the abovementioned measurements reached the specified values after bleaching. The AlBe-G removed the chlorophyll more efficiently compared to the FeBe-I, which was associated with the size of pores, yet both samples decolourized the oil adequately. The FeBe-I bentonite treated at 1 M oxalic acid presented maximum decolourization, which is associated with its high porosity. Moreover, low chlorophyll value and low colour were concurrently achieved by using the AlBe-G bentonite treated with 1 M oxalic acid as a bleaching earth.

Author Contributions: Supervision, M.T.; conceptualization, I.D.; writing—original draft preparation, D.T. All authors have read and agreed to the published version of the manuscript.

Funding: This research was funded by the Special Account for Research Funding (E.L.K.E.) of the National Technical University of Athens (N.T.U.A.) through doctoral fellowship.

Acknowledgments: The authors would like to thank IMERY S.A. and ELAIS Unilever Hellas S.A., for the supply of raw smectites and soybean oil, respectively.

Conflicts of Interest: The authors declare no conflict of interest.

References

1. Bergaya, F.; Theng, B.K.G.; Lagaly, G. *Handbook of Clay Science*, 1st ed.; Elsevier: Amsterdam, The Netherlands, 2008; p. 263.
2. Hussin, F.; Aroua, M.K.; Daud, W.M.A.W. Textural characteristics, surface chemistry and activation of bleaching earth: A review. *Chem. Eng. J.* **2011**, *170*, 90–106. [[CrossRef](#)]

3. Christidis, G.E.; Scott, P.W.; Dunham, A.C. Acid activation and bleaching capacity of bentonites from the islands of Milos and Chios, Aegean, Greece. *Appl. Clay Sci.* **1997**, *12*, 329–347. [[CrossRef](#)]
4. Önal, M.; Sarikaya, Y.; Alemdaroğlu, T.; Bozdoğan, I. The effect of acid activation on some physicochemical properties of a bentonite. *Turk. J. Chem.* **2002**, *26*, 409–416.
5. Tomić, Z.P.; Logar, V.P.; Babic, B.M.; Rogan, J.R.; Makreski, P. Comparison of structural, textural and thermal characteristics of pure and acid treated bentonites from Aleksinac and Petrovac (Serbia). *Spectrochim. Acta A* **2011**, *82*, 389–395. [[CrossRef](#)] [[PubMed](#)]
6. Kumar, P.; Jasra, R.V.; Bhat, T.S.G. Evolution of porosity and surface acidity in montmorillonite clay on acid activation. *Ind. Eng. Chem. Res.* **1995**, *34*, 1440–1448. [[CrossRef](#)]
7. Pesquera, C.; González, F.; Benito, I.; Blanco, C.; Mendioroz, S.; Pajares, J. Passivation of a montmorillonite by the silica created in acid activation. *J. Mater. Chem.* **1992**, *2*, 907–911. [[CrossRef](#)]
8. Gates, W.P.; Anderson, J.S.; Raven, M.D.; Churchman, G.J. Mineralogy of a bentonite from Miles, Queensland, Australia and characterisation of its acid activation products. *Appl. Clay Sci.* **2002**, *20*, 189–197. [[CrossRef](#)]
9. Madejová, J.; Bujdák, J.; Janek, M.; Komadel, P. Comparative FT-IR study of structural modifications during acid treatment of dioctahedral smectites and hectorite. *Spectrochim. Acta A* **1998**, *54*, 1397–1406. [[CrossRef](#)]
10. Babaki, H.; Salem, A.; Jafarizad, A. Kinetic model for the isothermal activation of bentonite by sulfuric acid. *Mater. Chem. Phys.* **2008**, *108*, 263–268. [[CrossRef](#)]
11. Tyagi, B.; Chudasama, C.D.; Jasra, R.V. Determination of structural modification in acid activated montmorillonite clay by FT-IR spectroscopy. *Spectrochim. Acta A* **2006**, *64*, 273–278. [[CrossRef](#)]
12. Welch, S.A.; Ullman, W.J. Feldspar dissolution in acidic and organic solutions: Compositional and pH dependence of dissolution rate. *Geochim. Cosmochim. Acta* **1996**, *60*, 2939–2948. [[CrossRef](#)]
13. Cama, J.; Ganor, J. The effects of organic acids on the dissolution of silicate minerals: A case study of oxalate catalysis of kaolinite dissolution. *Geochim. Cosmochim. Acta* **2006**, *70*, 2191–2209. [[CrossRef](#)]
14. Rozalen, M.; Huertas, F.J. Comparative effect of chrysotile leaching in nitric, sulfuric and oxalic acids at room temperature. *Chem. Geol.* **2013**, *352*, 134–142. [[CrossRef](#)]
15. Kong, M.; Huang, L.; Li, L.; Zhang, Z.; Zheng, S.; Wang, M.K. Effects of oxalic and citric acids on three clay minerals after incubation. *Appl. Clay Sci.* **2014**, *99*, 207–214. [[CrossRef](#)]
16. Irawan, S.; Samsuri, A. A study of iron removal from Sabah montmorillonite by extracting with organic acid. In Proceedings of the Regional Conference for Young Chemists USM, Penang, Malaysia, 13–14 April 2004.
17. Khan, A.; Naqvi, S.H.J.; Kazmi, M.A.; Ashraf, Z. Surface activation of fuller’s earth (bentonite clay) using organic acids. *Sci. Int.* **2015**, *27*, 329–332.
18. Taxiarchou, M.; Douni, I. The effect of oxalic acid activation on the bleaching properties of a bentonite from Milos Island, Greece. *Clay Miner.* **2014**, *49*, 541–549. [[CrossRef](#)]
19. Ramos, M.E.; Garcia-Palma, S.; Rozalen, M.; Johnston, C.T.; Huertas, F.J. Kinetics of montmorillonite dissolution, an experimental study of the effect of oxalate. *Chem. Geol.* **2014**, *363*, 283–292. [[CrossRef](#)]
20. Ramos, M.E.; Emiroglu, C.; García, D.; Sainz-Díaz, C.I.; Huertas, F.J. Modeling the Adsorption of Oxalate onto Montmorillonite. *Langmuir* **2015**, *31*, 11825–11834. [[CrossRef](#)]
21. Gupta, M.K. *Practical Guide to Vegetable Oil Processing*, 2nd ed.; Academic Press: London, UK; AOCS Press: London, UK, 2017; p. 129.
22. Balestri, S.; Beretta, S. *Poverty Eradication: Access to Land, Access to Food*; EduCatt: Milan, Italy, 2015; pp. 103–113.
23. Shahidi, F. *Bailey’s Industrial Oil and Fat Products*, 6th ed.; John Wiley and Sons Inc.: Hoboken, NJ, USA, 2005; Volumes 1–6, pp. 285–339.
24. Noyan, H.; Önal, M.; Sarikaya, Y. The effect of sulphuric acid activation on the crystallinity, surface area, porosity, surface acidity, and bleaching power of a bentonite. *Food Chem.* **2007**, *105*, 156–163. [[CrossRef](#)]
25. Didi, M.A.; Makhoukhi, B.; Azzouz, A.; Villemin, D. Colza oil bleaching through optimized acid activation of bentonite. A comparative study. *Appl. Clay Sci.* **2009**, *42*, 336–344. [[CrossRef](#)]
26. Karagüzel, C.; Çetinel, T.; Boylu, F.; Çinku, K.; Çelik, M.S. Activation of (Na, Ca)-bentonites with soda and MgO and their utilization as drilling mud. *Appl. Clay Sci.* **2010**, *48*, 398–404. [[CrossRef](#)]
27. Liua, Y.; Meib, Y.; Liuc, H.; Xu, D.; Peng, C. Identification and Assessment of Natural Sodium Bentonite. *Key Eng. Mater.* **2015**, *633*, 154–158. [[CrossRef](#)]
28. Šrodoň, J. Quantitative X-ray Diffraction Analysis of Clay-Bearing Rocks from Random Preparations. *Clays Clay Miner.* **2001**, *49*, 514–528. [[CrossRef](#)]
29. Köster, H.M.; Ehrlicher, U.; Gilg, H.A.; Jordan, R.; Murad, E.; Onnich, K. Mineralogical and chemical characteristics of five nontronites and Fe-rich smectites. *Clay Miner.* **1999**, *34*, 579–599. [[CrossRef](#)]
30. Temuujin, J.; Jadambaa, T.; Burmaa, G.; Erdenechimeg, S.; Amarsanaa, J.; MacKenzie, K.J.D. Characterisation of acid activated montmorillonite clay from Tuulant (Mongolia). *Ceram. Int.* **2004**, *30*, 251–255. [[CrossRef](#)]
31. Tabak, A.; Afsin, B.; Caglar, B.; Koksall, E. Characterization and pillaring of a Turkish bentonite (Resadiye). *J. Colloid Interface Sci.* **2007**, *313*, 5–11. [[CrossRef](#)] [[PubMed](#)]
32. Goodman, B.A. A Mössbauer and I.R. Spectroscopic Study of the Structure of Nontronite. *Clays Clay Miner.* **1976**, *24*, 53–59. [[CrossRef](#)]

33. Frost, R.L.; Kloprogge, J.T.; Ding, Z. Near-infrared spectroscopic study of nontronites and ferruginous smectite. *Spectrochim. Acta A* **2002**, *58*, 1657–1668. [[CrossRef](#)]
34. Roy, M.; Meena, S.K.; Kusurkar, T.S.; Singh, S.K.; Sethy, N.K.; Bhargava, K.; Sarkar, S.; Das, M. Carbondioxide gating in silk cocoon. *Biointerphases*. **2012**, *7*, 45. [[CrossRef](#)]
35. Sing, K.S.W.; Everett, D.H.; Haul, R.A.W.; Moscou, L.; Pierotti, R.A.; Rouquérol, J.; Siemieniewska, T. Reporting physisorption data for gas/solid systems with special reference to the determination of surface area and porosity. *Pure Appl. Chem.* **1985**, *57*, 603–619. [[CrossRef](#)]
36. Francisco, R.; Díaz, V.; Santos, P.S. Studies on the acid activation of Brazilian smectitic clays. *Quim. Nova* **2001**, *24*, 345–353.
37. Sariođlan, Ş.; Yüzer, H.; Koral, M. Acid Activation and Bleaching Performance of Turkish (Somas) Bentonite in Crude Soybean Oil. *Part. Sci. Technol.* **2010**, *28*, 298–308. [[CrossRef](#)]
38. Mokaya, R.; Jones, W.; Davies, M.E.; Whittle, M.E. Chlorophyll adsorption by alumina-pillared acid-activated clays. *J. Am. Oil Chem. Soc.* **1993**, *70*, 241–244. [[CrossRef](#)]
39. Mackinney, G.; Chichester, C.O. The Color Problem in Foods. In *Advances in Food Research*, 1st ed.; Mrak, E.M., Stewart, G.F., Eds.; Academic Press Inc.: New York, NY, USA, 1954; Volume 5, pp. 301–351.
40. Boki, K.; Kubo, M.; Kawasaki, N.; Mori, H. Adsorption Isotherms of Pigments from Alkali Refined Vegetable Oils with Clay Minerals. *J. Am. Oil Chem. Soc.* **1992**, *69*, 372–378. [[CrossRef](#)]
41. Henache, Z.; Boukerroui, A.; Kashi, I. Modeling of the soybean oil bleaching and optimization of its conditions in the refining process for environmental interest. *Nova Biotechnol. Chim.* **2018**, *17*, 48–57. [[CrossRef](#)]